

Thermal photon-IMF anticorrelation: a signal of prompt multifragmentation?

R. Alba,¹ C. Agodi,¹ C. Maiolino,¹ A. Del Zoppo,¹ M. Colonna,¹ G. Bellia,^{1,2} M. Bruno,³
N. Colonna,⁴ R. Coniglione,¹ M. D'Agostino,³ M.L. Fiandri,³ P. Finocchiaro,¹ F. Gramegna,⁵
I. Iori,⁶ K. Loukachine,¹ G.V. Margagliotti,⁷ P.F. Mastinu,⁵ P.M. Milazzo,⁷ E. Migneco,^{1,2}
A. Moroni,⁶ P. Piattelli,¹ R. Rui,⁷ D. Santonocito,¹ P. Sapienza,¹ G. Vannini³
(1) INFN - Laboratori Nazionali del Sud, Via S. Sofia 62, I-95123 Catania (ITALY)
(2) Dipartimento di Fisica e Astronomia dell'Università, Catania (ITALY)
(3) INFN and Dipartimento di Fisica dell'Università, Bologna (ITALY)
(4) INFN, Bari (ITALY)
(5) INFN - Laboratori Nazionali di Legnaro, Legnaro (ITALY)
(6) INFN and Dipartimento di Fisica dell'Università, Milano (ITALY) and
(7) INFN and Dipartimento di Fisica dell'Università, Trieste (ITALY)

(Dated: November 10, 2018)

The mechanism responsible for IMF emission in central $^{58}\text{Ni} + ^{197}\text{Au}$ reactions at 30 and 45 MeV/nucleon is investigated by looking at the thermal bremsstrahlung photon production. An IMF - photon anticorrelation signal is observed, for central collisions, at 45 MeV/nucleon with IMF velocity around the center of mass value. This observation is proposed as an evidence for prompt nuclear fragmentation events.

Heavy ion collisions at intermediate energy offer the possibility to access states of nuclear matter in which density and temperature conditions, far from normal ones, give rise to a variety of new phenomena.

For instance, when the nuclear matter is compressed, two body nucleon-nucleon collisions are favored and this leads to an enhanced production of incoherent bremsstrahlung photons. In the Fermi energy domain, two main sources of incoherent bremsstrahlung photons ($E_\gamma > 25$ MeV) have been observed. In the first one, located in the early compression phase of the reaction and in the overlap region of the two colliding nuclei [1, 2, 3, 4, 5, 6] high energy bremsstrahlung photons are produced in first chance collisions of projectile protons (neutrons) on target neutrons (protons) [4, 7, 8]. These are called *direct* photons. In the second one, that as indicated by interferometry measurements [9] has a larger extension in space-time with respect to the direct one [10], bremsstrahlung photons are still produced in p-n collisions but in a phase of the reaction in which the identity of projectile (target) nucleons is lost. This results in a smaller photon energy, that reflects the temperature evolution of the composite system [11, 12]. These are called *thermal* photons. A possible interpretation of this phenomenon, substantiated by quantitative estimates [10, 12], is provided by BUU calculations [13]. These studies associate thermal photon emission with monopole oscillations (a second compression phase) experienced by the composite system. This scenario appears quite appealing since it opens the possibility to extract information on the nuclear matter compressibility and equation of state.

Reactions at intermediate energies are also accompanied by a copious production of IMF's (fragments with charge $3 \leq Z \leq 20$), the so-called multifragmentation [14]. Whether such a process is a phenomenon consist-

ing in the prompt disintegration of the system during the expansion phase that follows the initial collisional shock [15, 16, 17, 18, 19, 20, 21] or it occurs at larger times, as a late deexcitation of a hot thermalized system [22], is still an open problem.

In this work we investigate experimentally, in heavy ion central collisions, the production of IMF's and thermal photons inside the same reaction event. The observable adopted in our study is the thermal photon-IMF multiplicity correlation factor

$$(1 + R)_{th} = \frac{\langle m_\gamma^{th} \cdot m_{IMF} \rangle}{\langle m_\gamma^{th} \rangle \cdot \langle m_{IMF} \rangle} \quad (1)$$

m_γ^{th} being mostly 0 or 1.

Lack of correlation indicates unambiguously that IMF and thermal photon production mechanisms are compatible and independent. This is the case of IMF emission in the late de-excitation of a hot heavy system, indicated as HHS in the following, that is formed during the reaction path, and that can be identified as a composite source in central collisions or as a target remnant in the other cases. On the other hand, if anticorrelation is observed, IMF and thermal photon emissions are incompatible mechanisms, like in a scenario where the prompt disintegration of the system, expected in violent collisions [15, 16, 17, 18, 19, 20, 21], inhibits the formation of the thermal photon source, i.e. the HHS. The value of the factor (1) equals zero in the case of prompt complete disintegration of the system into small fragments (production of the coincident thermal photon totally inhibited), while it equals 1 in the case of late statistical fragmentation of the HHS, if the energy balance does not introduce strong constraints.

We have studied the reaction $^{58}\text{Ni} + ^{197}\text{Au}$ at two bombarding energies, 30 and 45 MeV/nucleon. This choice

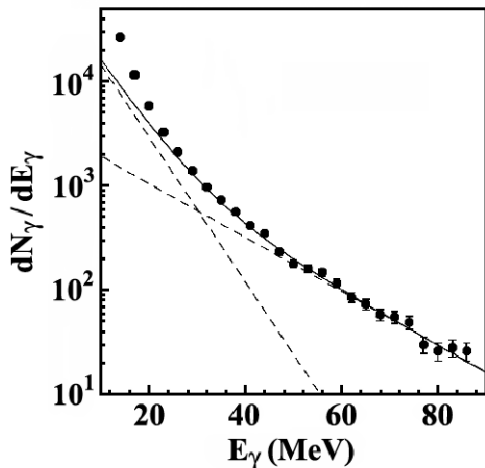


FIG. 1: *Experimental photon energy spectrum for Ni + Au at 45 MeV/nucleon, central reactions. Dashed lines: thermal and direct contributions to the fit (full line).*

has been motivated by the need of a compromise between the possibility to reach enough compression in the collision and a significant thermal to direct photon ratio, that has been observed to decrease with increasing bombarding energy [12]. Moreover, as we will see, this study performed at two bombarding energies, allows to rule out that the anticorrelation signal is a trivial energy balance effect which accounts for the energy taken by the photon.

The experiment has been performed at Laboratori Nazionali del Sud bombarding a 2.5 mg/cm² thick Au target with ⁵⁸Ni beams at 30 and 45 MeV/nucleon delivered by the Tandem and Superconductive Cyclotron (CS) acceleration system. Since nuclear bremsstrahlung is an extremely rare process, this study has required the combined use of MEDEA [23] and MULTICS [24] sophisticated and extensive multidetector arrays. MEDEA is a ball, built with 180 BaF₂, each 20 cm thick, placed at 22 cm from the target, which covers the polar angles from 30° to 170°. The BaF₂ permit to detect and identify light charged particles and photons. The MULTICS array consists of 55 telescopes, each formed by an ionization chamber, a silicon detector and a CsI crystal, located at 50 cm from the target, and allows the identification of charged particles up to Z=83. The total geometric acceptance is larger than 90% of 4π.

To select the events as a function of centrality we have used the charged particle multiplicity, converted into impact parameter according to the geometrical prescriptions of [25]. In the following analysis we will consider, as central events, the impact parameter region $b/b_{max} < 0.35$. This corresponds to about 10⁷ events at the larger beam energy (45 MeV/nucleon). In this class of events the average IMF multiplicity is equal to $0.623 \pm 4 \cdot 10^{-3}$.

Fig.1 shows the experimental photon energy spectrum for the system ⁵⁸Ni + ¹⁹⁷Au at 45 MeV/nucleon, obtained in central events. The photon spectrum deviates from a pure exponential dependence on E_γ . Such a deviation is consistent with the presence of two contributions, each one having a dependence of the type $\exp -\frac{E_\gamma}{E_0}$ on E_γ but with very different inverse slope parameters E_0 [26]. The two component fit to the data is also shown in Fig.1. The component with the largest E_0 can be related to the direct photons produced in first chance two-body collisions between nucleons coming from the initially separated projectile and target Fermi clouds in macroscopic relative motion. In this case, for a given projectile-target combination, E_0 only depends on the incident energy. The small E_0 component is associated with the thermal photons, the experimental values of E_0 being related to the temperature of the HHS [27, 28]. At low energies ($E_\gamma < 20$ MeV) one observes also statistical photons emitted from the excited products.

For both incident energies and selected impact parameter b bins, a simultaneous fit to the photon energy and angular distributions allowed us to determine the relevant characteristics of the thermal photon source [26]. Inverse slope parameter values of the order of 4-5 MeV, a source velocity approaching that of the nucleus-nucleus center of mass with increasing centrality and a very small anisotropy have been deduced in agreement with [11, 12]. Thermal photons are present in all the spectra of this experiment indicating that in the studied reactions the HHS is formed in a significant number of events.

It is evident from Fig.1 that thermal photons cannot be isolated completely from direct photons or statistical photons and therefore the experimental correlation factor is the sum of the correlation factors of the IMF's with thermal, direct and statistical photons, weighted by the relative intensities:

$$(1 + R)_{exp} = \frac{I_\gamma^{th}}{I_\gamma} \cdot (1 + R)_{th} + \frac{I_\gamma^{dir}}{I_\gamma} \cdot (1 + R)_{dir} + \frac{I_\gamma^{stat}}{I_\gamma} \cdot (1 + R)_{stat}. \quad (2)$$

Let us focus on central collisions, in which about 8500 and 3000 γ 's with energy larger than 30 MeV have been collected at the incident energy of 45 MeV/nucleon and 30 MeV/nucleon, respectively. The correlation factor (2) has been evaluated as a function of the photon energy. Namely we consider all photons with energy greater than a threshold E_γ and calculate the correlation factor as a function of E_γ . We have considered two windows for the IMF's velocity: W_{cm} , that extends up to $\beta \approx 0.1$ and includes the nucleus-nucleus center of mass velocity, i.e. the window where the thermal photon source is localized, and W_h , that includes all IMF's with higher velocity ($\beta > 0.1$).

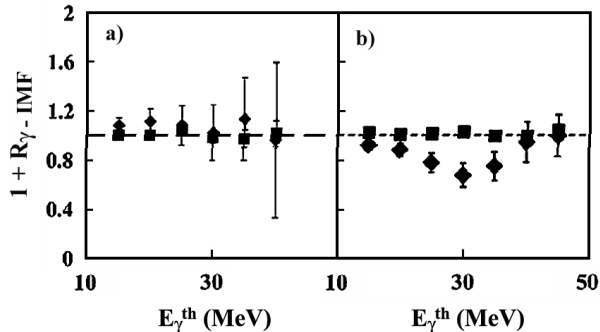


FIG. 2: Experimental photon - IMF correlation factors versus the threshold E_γ (see text), for IMF's in two velocity windows: W_{cm} (diamonds), W_h (squares). Data are shown at 30 MeV/nucleon (a) and 45 MeV/nucleon (b), for central collisions.

The results obtained at 30 and 45 MeV/nucleon are displayed in Fig.2.

At 45 MeV/nucleon, for IMF's in the W_{cm} window, a clear anticorrelation signal appears in the region where thermal photon contribution is more abundant. This observation is the type of signal strongly expected in presence of prompt fragmentation, that competes with the HHS formation and inhibits thermal photon production. The signal disappears at low and high gamma energy due to the overbalance of the other photon production mechanisms (see Eq.(2)), that also dims the true anticorrelation signal. The IMF's with a larger velocity (in the W_h window), mostly coming from pre-equilibrium emission in the very early stage of the collision, do not appear correlated with the thermal photon production, as expected, because they are associated with a different emission source. At 30 MeV/nucleon, within error bars, $1 + R$ is always equal to one, both in the window W_h and in the window W_{cm} . In this second case, the absence of the correlation can be seen as a signal of independent production of gamma's and IMF's, due to the dominance of late fragmentation of the HHS.

We underline that the difference observed at the two beam energies cannot be ascribed to a trivial effect of the energy conservation, because such effect works in the opposite direction and, due to the energy carried away by the photon, should result in an anticorrelation signal stronger at 30 MeV/nucleon than at 45 MeV/nucleon.

At 45 MeV/nucleon the analysis has been performed also as a function of the impact parameter for a γ energy bin in which the thermal photon contribution is large ($25 \text{ MeV} < E_\gamma < 40 \text{ MeV}$) and for IMF's in W_{cm} . The results are shown in Fig.3. It can be seen that the anticorrelation increases with the violence of the collision showing that the contribution of IMF's promptly emitted grows with the centrality of the collision. The same analysis could

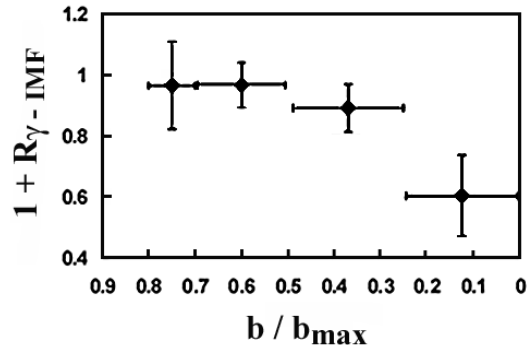


FIG. 3: Thermal photon - IMF correlation factors, for IMF's in the velocity window W_{cm} , as a function of impact parameter. Data are shown at 45 MeV/nucleon.

not be done at 30 MeV/nucleon for lack of statistics.

A rough evaluation of the significance of the differences observed in Fig.2 between the results at 30 and 45 MeV/nucleon has been made according to the Kolmogorov test. The two trends have been found different at a confidence level of 95%, in spite of the quite large error bars affecting the 30 MeV/nucleon data.

We have estimated the probability that the observed anticorrelation could be due to multiple firing of the detectors, that could cause the lack of γ 's when high LCP multiplicities (as in central collisions) are detected in the BaF_2 arrays. For the detected multiplicities (< 20) and the MEDEA granularity, this probability results negligible and affects the correlation signal by less than 3%.

Prompt fragmentation processes have been recently studied in the context of dynamical models incorporating the effects of many-body correlations and fluctuations [19, 21]. To check the interpretation proposed above, stochastic mean field simulations [19] have been performed in the case of the reactions studied here at both incident energies, for central impact parameters ($b/b_{max} = 0.17$ in the calculations). A soft EOS, with compressibility modulus $K = 200 \text{ MeV}$, has been used. A stiffer behaviour of the EOS would move the onset of prompt multifragmentation to higher beam energies.

It appears that the primary fragment charge distributions predicted by these calculations are completely different for the two energies considered (Fig.4a), indicating the dominant role of prompt multifragmentation only at 45 MeV/nucleon. In fact, at 30 MeV/nucleon in most of the events, after the initial collisional shock and the subsequent expansion, the system compacts again leading to the formation of a HHS within a narrow interval of charge around $Z = 80$. On the other hand, at 45 MeV/nucleon this happens only in a small fraction of the total number of events, leading to HHS's with charge $Z \geq 70$, while prompt IMF formation is mostly observed. The final charge distribution, after evaporation of the primary

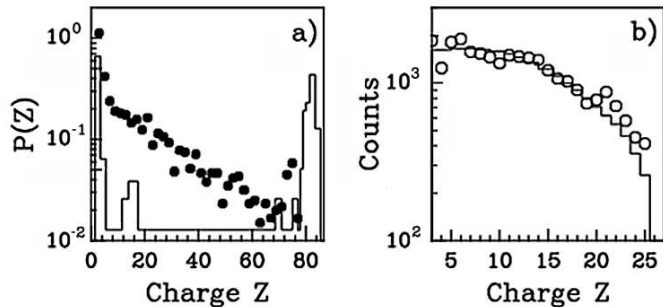


FIG. 4: a) Primary fragment Z -distributions from stochastic mean-field calculations at 30 MeV/nucleon (full line) and 45 MeV/nucleon (filled circles). b) Comparison between experimental charge distribution, at 45 MeV/A (open circles), and the final filtered simulations (full line). See text for details.

products [29], has been calculated for both energies. At 30 MeV/nucleon IMF's are mainly produced by the statistical decay of the HHS. Instead, at 45 MeV/nucleon the charge distribution is almost not affected by the secondary decay. In Fig.4b we show the final filtered distribution compared to the experimental data. The two distributions have been normalized to the same area in the region $4 < Z < 25$. The agreement is quite satisfactory. Moreover, the calculated filtered IMF's multiplicities reproduce the experimental ones within 30%, a good agreement if we consider that the calculations are not impact parameter averaged.

Since, as discussed above, prompt IMF's and HHS are expected to be anticorrelated as IMF's and thermal photons, we have calculated the multiplicity correlation factor

$$(1 + R)_{HHS} = \frac{\langle m_{HHS} \cdot m_{IMF} \rangle}{\langle m_{HHS} \rangle \cdot \langle m_{IMF} \rangle}, \quad (3)$$

the possible values of m_{HHS} being only 0 or 1. As intuitively expected looking at the distributions in Fig.4a, the anticorrelation results weak at 30 MeV/nucleon ($(1 + R)_{HHS} = 0.97$) and becomes stronger at 45 MeV/nucleon ($(1 + R)_{HHS} = 0.5$).

Hence simulations follow the same trend as observed in the experimental data, supporting the occurrence of prompt multifragmentation at the highest energy. The prompt character of IMF emission has been also assessed in other recent experimental observations [30, 31].

In summary, in this work we investigate the correlation factor between thermal photons and IMF's as an indicator of the mechanism and of the time scales of nuclear fragmentation. For central Ni+Au collisions the observation of an anticorrelation with IMF's in the center of mass velocity window appears as a signal of prompt multifragmentation at 45 MeV/nucleon. Dynamical calcula-

tions based on the stochastic mean-field approach, with a soft EOS, including statistical de-excitation of the primary HHS, also indicate the dominance of prompt IMF emission in central collisions at 45 MeV/nucleon.

In conclusion, we believe that at the highest bombarding energy studied in this experiment we have observed different processes which mark significantly the dynamical evolution of violent nucleus-nucleus collisions: the production of direct photons in the primordial compressed phase, the onset of prompt fragmentation during the expansion of the system and the competition with a resilience of the nuclear system towards a composite source formation, responsible for the production of thermal photons.

We thank the LNS staff for the beam quality and for the support during the experiment.

-
- [1] H.Nifenecker and J.A.Pinston, Prog.Part.Nucl.Phys. **23**, 271 (1989).
 - [2] E.Migneco *et al.*, Phys.Lett. B **298**, 46 (1993).
 - [3] G.Martinez *et al.*, Phys.Lett. B **334**, 23 (1994).
 - [4] P.Sapienza *et al.*, Phys.Rev.Lett. **73**, 1769 (1994).
 - [5] H.Nifenecker and J.P.Bondorf, Nucl.Phys. **A442**, 478 (1985).
 - [6] W.Cassing *et al.*, Phys.Rep. **188**, 365 (1990).
 - [7] W.Bauer *et al.*, Nucl.Phys. **A456**, 159 (1986).
 - [8] T.Biro *et al.*, Nucl.Phys. **A475**, 579 (1987).
 - [9] F.M.Marques *et al.*, Phys.Rev.Lett. **73**, 34 (1994).
 - [10] F.M.Marques *et al.*, Phys.Lett. B **349**, 30 (1995).
 - [11] A.Schubert *et al.*, Phys.Rev.Lett. **72**, 1608 (1994).
 - [12] G.Martinez *et al.*, Phys.Lett. B **349**, 23 (1995).
 - [13] A.Bonasera *et al.*, Phys.Lett. B **246**, 337 (1990); A.Guarnera *et al.*, Phys.Lett. B **373**, 267 (1996).
 - [14] see e.g. D.R.Bowman *et al.*, Phys.Rev.Lett. **67**, 1527 (1991) and refs therein.
 - [15] J.Aichelin, Phys.Rep. **202**, 223 (1991).
 - [16] J.P.Bondorf *et al.*, Phys.Rep. **257**, 133 (1995).
 - [17] D.H.E.Gross, Rep.Prog.Phys. **53**, 605 (1990).
 - [18] D.Hahn and H.Stocker, Nucl.Phys. **A476**, 718 (1988).
 - [19] Ph.Chomaz, M.Colonna and J.Randrup, Phys. Rep. **389**, 263-440 (2004); M.Colonna *et al.*, Nucl. Phys. **A742**, 337-347 (2004).
 - [20] W.A.Friedman, Phys.Rev. **C 42**, 667 (1990).
 - [21] A.Ono, Phys. Rev. **C 59**, 853 (1999).
 - [22] L.G.Moretto *et al.*, Phys. Rep. **287**, 250 (1997).
 - [23] E.Migneco *et al.*, Nucl.Inst.Methods A **314**, 31 (1992).
 - [24] I.Iori *et al.*, Nucl.Inst.Methods A **325**, 458 (1993).
 - [25] C.Cavata *et al.*, Phys.Rev. **C 42**, 1760 (1990).
 - [26] R.Alba *et al.*, Nucl.Phys. **A654**, 761c (1999) and Nucl.Phys. **A681**, 339c (2001).
 - [27] D. D'Enterria *et al.*, Phys.Rev.Lett. **87**, 022701 (2001).
 - [28] D. D'Enterria *et al.*, Phys.Lett. **538**, 27 (2002).
 - [29] D.Durand, Nucl.Phys. **A541**, 266 (1992).
 - [30] G.Tabacaru *et al.*, Eur. Phys.J. **A18**, 103 (2003).
 - [31] M.D'Agostino *et al.*, Nucl. Phys. **A699**, 795 (2002).